SSRG International Journal of Electronics and Communication Engineering
ISSN: 2348-8549/ https://doi.org/10.14445/23488549/IJECE-V12I4P112

Volume 12 Issue 4, 132-141, April 2025

Original Article

Cutting-Edge Image Processing of Lower Gastrointestinal Track Using Deep Learning

S. Vasudevan[1], Vediyappan Govindan[2], Haewon Byeon[3]

[1,2]Department of Mathematics, Hindustan Institute of Technology and Science, Chennai, Tamilnadu, India.
[3]Worker's Care & Digital Health Lab, Department of Future Technology, Korea University of Technology and Education, Cheonan, South Korea.

[2]Corresponding Author : govindoviya@gmail.com

Received: 09 February 2025 Revised: 11 March 2025 Accepted: 12 April 2025 Published: 29 April 2025

Abstract *- Lower Gastrointestinal (GI) problems rely heavily on medical imaging for diagnosis and therapy. The Kvasir dataset is useful for medical imaging research, particularly in gastroenterology. The dataset comprises high-quality movies and pictures captured during endoscopic operations, which depict the gastrointestinal tract, including the stomach, duodenum, colon, and oesophagus. The data was collected through Kaggle. The frequent susceptibility of these pictures to noise and distortions may hinder accurate analysis. In this article, we report a new method using sophisticated mathematical analysis to improve and brighten pictures of the Lower Gastrointestinal (GI) tract, such as pylorus, normal-cecum, and ulcerative colitis images. Our goal was to enhance the picture quality through the use of various statistical filters, Gaussian functions, the Fast Fourier Transform (FFT), and the Inverse Fast Fourier Transform (IFFT). This would enable more precise classification and detection. According to our investigation, adaptive mean filtering plus Gaussian correction performed noticeably better than conventional bi-cubic filtering. On the other hand, the bi-cubic filter had a PSNR of 42.06 and an MSE of 4.04. The combined filter technique, on the other hand, had a PSNR of 49.44 and an MSE of 0.73. The results show that using both the adaptive mean filter and the Gaussian correction approach together is the best way to improve images for lower GI tract exams. This makes the images clearer and more detailed. Additionally, the combined filter's improved image processing makes lower GI structures easier to see and understand, which helps doctors diagnose patients and plan treatments. Overall, our results highlight the value of using sophisticated filter approaches to improve image processing in lower gastrointestinal imaging, with the combined filter showing itself to be the best option for raising diagnostic precision and picture quality.*

Keywords *- Computer Vision, Deep Learning, Image Analysis, Partial Differential Equation, Python.*

1. Introduction

Diagnostic medicine has radically transformed in recent years because of developments in medical imaging technology and the strength of deep learning algorithms. These developments have been very beneficial for some fields, such as Lower Gastrointestinal (GI) image processing. When it comes to the detection and treatment of a variety of gastrointestinal conditions, including gastrointestinal bleeding, inflammatory bowel disease, and colorectal cancer, lower GI imaging is essential [1]. However, clinician judgment has always played a major role in interpreting lower GI pictures, which can be laborious and subjective. To overcome these issues, it is necessary to develop automated and improved image analysis tools for lower GI pictures that utilize deep learning techniques and other computational methodologies. These methods take advantage of deep learning models' capacity to extract significant characteristics and patterns from complicated pictures [2] and the enormous volumes of data accessible from medical imaging archives. In this study, we thoroughly evaluate and analyze the most recent methods for improved image processing of lower gastrointestinal pictures. We delve into various deep learning architectures, such as Convolutional Neural Networks (CNNs) [3], tailoring them to the distinct characteristics of lower gravity photos. To further improve the precision and effectiveness of lower GI image analysis, we also investigate integrating other cutting-edge computational methods, such as image segmentation, feature extraction, and image registration. We also draw attention to the intriguing directions that remain for further study and development, including the introduction of real-time feedback mechanisms for clinical decision support and the integration of multimodal imaging data. All things considered, combining deep learning with other computer methods can completely transform the interpretation of lower gastrointestinal pictures, ultimately resulting in more precise diagnoses, individualized treatment plans, and better patient outcomes. Our goal in writing this work is to stimulate more research in this vital field of medicine by offering insights into the state of improved image analysis in lower GI imaging today.

2. About the Data

2.1. Second-Order Heading

We conducted our computational studies using Google Colab, a cloud-based platform that provides robust computational capabilities. More specifically, we utilized the NVIDIA Tesla T4 GPU available in the Colab environment to accelerate our data-intensive workloads and deep learning models [4]. The Colab environment's 16 GB of RAM and 100 GB of disk space allowed us to handle large datasets effectively.

3. Analysis on Kvasir

3.1. Image Smoothening

3.1.1. Average Filter

One popular image processing method for reducing noise and producing a more aesthetically attractive outcome is picture smoothing. Smoothening can improve picture clarity for analysis or diagnosis when used on medical imaging datasets such as Kvasir, which includes gastrointestinal endoscopic images.

(m-1, n-1)	(m-1, n)	(m-1, n+1)
(m, n-1)	(m, n)	(m, n+1)
(m+1, n-1)	(m+1, n)	(m+1, n+1)

$$\boldsymbol{Pixel(m,n) = data(m * width + n)}$$

$$\boldsymbol{Pixel\ (i,j) = \sum_{x=-1}^{1}\sum_{y=-1}^{1} initialPixel(m+x,n+y)/9}$$

$$\boldsymbol{Pixel\ (i,j) = \sum_{x=-1}^{1}\sum_{y=-1}^{1} initialPixel(m+x,n+y)/25}$$

Eight pixels encircle every pixel in the image, except the pixels at the margins, which are disregarded. Then using, the average of the nine pixels in the figure is used to recalculate each pixel's value.

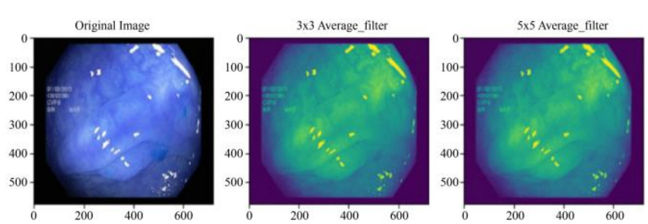

1 Image smoothening along with different filters

To reduce the disparities between each pixel and improve the image's smoothness, we substitute the average value [5] of the surrounding eight pixels and the pixel itself for the values shown in Figure 1 on the cantered picture. However, the denoising process not only fails to protect the picture details but also erodes them, resulting in a blurred image. Since the right-side image now averages each pixel over the 24 surrounding pixels, the difference in pixel density over the entire image is lower. As a result, the 5x5 mask's processed picture is visibly smoother and more blurry than the 3x3 mask. Additionally, we obtained mostly unique pixels.

3.1.2. Median Filter

In this section, the median filter substitutes the median value of the intensities within a specified neighborhood for each pixel's value. We replace each pixel's value with the median of the next eight pixels, thereby reducing disparities among all pixels and smoothing the image. After noise reduction, the objects' edges are sharper in the median filter than in the average filter shown in Figure 2. Furthermore, because it only processes the target pixel once, there is a greater variation between pixels.

Fig. 2 Median filter applied on the kvasir data

In medical photographs, the use of median and average filters might cause undesired distortion or blurring of important features, which could jeopardize the accuracy of the diagnosis. These filters might introduce artifacts or smooth down significant characteristics, which could lead to physicians making inaccurate evaluations.

Rather, medical imaging usually uses more advanced techniques designed to guarantee diagnostic accuracy and preserve minute features. Improper use of filters on medical photos might have detrimental effects on patient care and diagnosis precision.

3.2. Image Reduction

In this filter, the scale to be reduced is and the original picture size is m*n, and the scale to reduce is $\boldsymbol{f(x)\ where\ (0 < f(x) < 1}$, and the output size will be $\boldsymbol{(m * f(x)) * (n * f(x))}$ shown in Figure 3.

X	1/f(x)		
X	X	X	X
1/f(x)	X	X	X
X	X	X	X

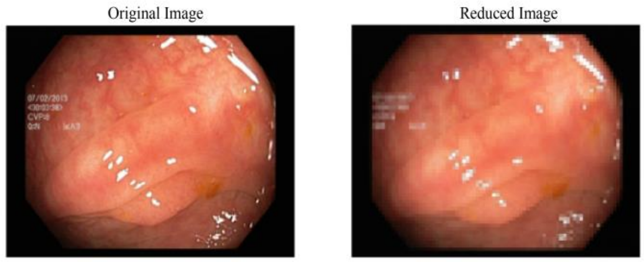

Fig. 3 Image reduction applied on pylorus data

Because of their lower resolution, medical photographs that have undergone image reduction may lose important diagnostic information. The accuracy of medical diagnosis may be impacted by the reduction process [6], which may result in the loss of minute information and minor anomalies. Maintaining high picture resolution is essential for accurate analysis and interpretation in medical imaging.

3.3. Image Sharpening

3.3.1. Median Filter

In the laplacian operator, picture sharpening is a widely used method in image processing. To calculate the local fluctuation of intensity in a picture, one can utilize the

Laplacian operator, a second-order differential operator. Enhancing these differences makes the image look crisper, as shown in Figure 4.

$$\boldsymbol{Laplace = \frac{\partial^2 f}{\partial x^2} + \frac{\partial^2 f}{\partial y^2}}$$

We get the difference from the Laplace Operator.

$$\boldsymbol{\nabla^2 f(x,y) = 4f(x,y) - f(x+1,y) - f(x-1,y) - f(x,y+1) - f(x,y-1)}$$

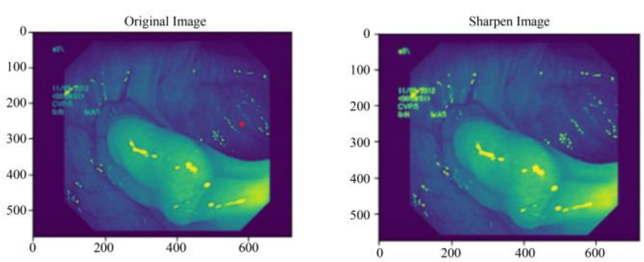

Fig. 4 Sharpening the edges using the laplace operator

The Laplacian filter draws attention to sharp contrasts in a picture, such as borders and edges. This may improve the visibility of anatomical features, lesions, polyps, or other anomalies in endoscopic images from the KVASIR dataset.

The Laplacian filter may enhance noise in the pictures, such as speckle noise or artifacts from the endoscopic technique, which might result in a loss of image quality or the introduction of misleading features.

3.3.2. Median Filter

In this session, edge detection is the main use of the Sobel operator. It computes the image's gradient at each pixel to find edges in both the horizontal and vertical axes.

$$\boldsymbol{\nabla f = gradient(f) = \begin{bmatrix} g_x \\ g_y \end{bmatrix}}$$

$$\boldsymbol{\nabla f = \begin{bmatrix} \partial f/_{\partial x} \\ \partial f/_{\partial y} \end{bmatrix}}$$

Then, combining the Horizontal and the Vertical Gradient,

$$\boldsymbol{G = \sqrt[2]{G_x^2 + G_y^2}}$$

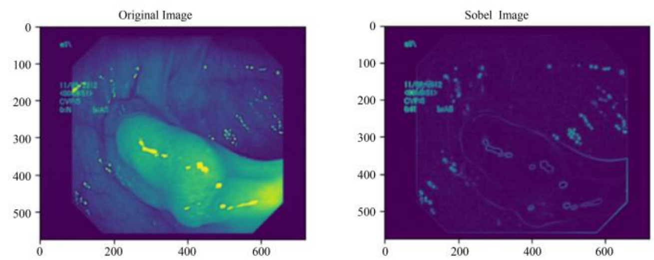

Fig. 5 Edge detection using the sobel operator

Following differentiation, the edge place's absolute value is quite big, whereas the flat place's value is nearly zero. However, the recovered picture contours are not always sufficient since the Sobel operator does not strictly separate the image's main body from its backdrop [7]. Regarding noise, the Sobel operator is less sensitive than the Laplacian operator, as shown in Figure 5. It can deliver edge detection findings that are more dependable and fluid.

The application's particular needs will determine whether Laplace or Sobel operators are best for image sharpening in medical photos. The Sobel operator computes gradients to highlight edges, but the Laplace operator effectively improves edges and fine details. However, small features must be preserved in medical imaging, which is why the Laplace operator is more appropriate since it can highlight minute structures without drawing attention to noise. Because of its gradient calculation, the Sobel operator may amplify noise, compromising the diagnostic precision of medical pictures.

3.4. Gamma Correction

In this part, Gamma correction, often referred to as gamma adjustment or gamma transformation, is a nonlinear process used to alter the brightness or luminance levels in digital photographs. To account for the nonlinear reaction, the pixel values of the pylorus must be changed. The properties of the Cathode-Ray Tube (CRT) monitor [8], which have a nonlinear connection between the input voltage and the brightness of the projected picture, are where the idea of gamma correction originated. The power-law function is frequently used to characterize the relationship:

Converting the pixel into the real number and normalizing it $(\boldsymbol{f}+\mathbf{0.5})/\mathbf{255}$ where f is the original pixel value.

$$\boldsymbol{Gamma\ correction} = \boldsymbol{f}_{\boldsymbol{c}}^{\boldsymbol{\gamma}}, \quad \boldsymbol{Where\ c}\ \&\ \boldsymbol{\gamma\ are\ constant}$$

Finally, deformalize the corrected value by taking the inverse value.

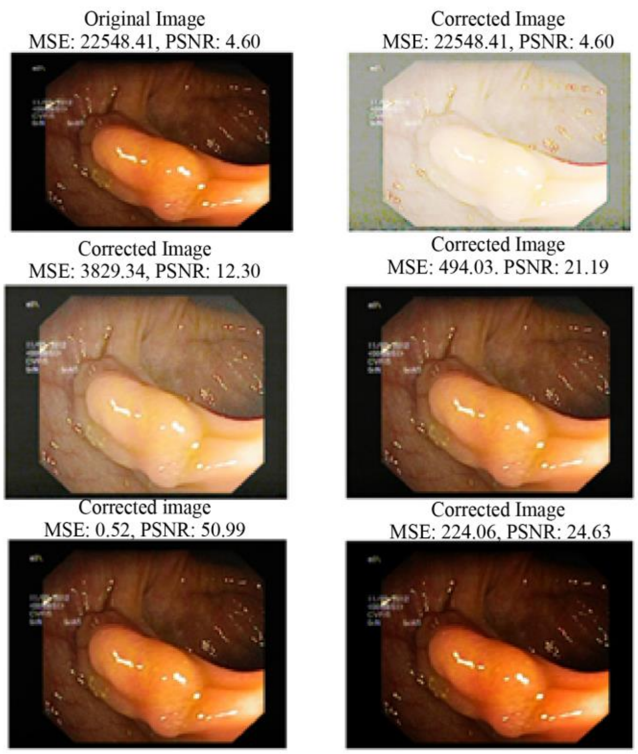

Fig. 6 Gamma correction along with different gamma value

Metrics like PSNR (Peak Signal-to-Noise Ratio) and MSE (Mean Squared Error) are frequently used to assess how well processed or reconstructed pictures compare to their originals.

The Mean Squared Error (MSE) calculates the difference between the original image and the processed (or reconstructed) picture. It is computed by averaging the respective pixel values of the two pictures over all pixels and then computing the square of the difference between those values. In terms of math, MSE is computed as follows:

$$\boldsymbol{MSE} = \frac{\mathbf{1}}{\boldsymbol{mn}} \sum_{\boldsymbol{i}=\mathbf{0}}^{\boldsymbol{m}-\mathbf{1}} \sum_{\boldsymbol{j}=\mathbf{0}}^{\boldsymbol{n}-\mathbf{1}} (\boldsymbol{Orijinal}(\boldsymbol{i},\boldsymbol{j}) - \boldsymbol{Processed}(\boldsymbol{i},\boldsymbol{j}))^{\mathbf{2}}$$

The ratio of a signal's maximal potential strength to the amount of corrupting noise that degrades the representational fidelity is called PSNR. PSNR is frequently used in image processing to assess the effectiveness of compression or reconstruction techniques. The formula for PSNR is as follows:

$$\boldsymbol{PSNR} = \mathbf{10} * \log_{\mathbf{10}}\left(\frac{\boldsymbol{MAX}^{\mathbf{2}}}{\boldsymbol{MSE}}\right)$$

With very little loss of picture quality, the processed pylorus image resembles the original with an MSE of 0.52 and a PSNR of 50.99. These results indicate that, in the context of KVASIR (pylorus) pictures shown in Figure 6, the algorithm employed for gamma correction or any other image enhancement approach has successfully enhanced the image quality, making it appropriate for additional analysis and diagnosis. Gamma correction improves the visual quality of images by adjusting the brightness and contrast. In the Kvasir dataset, a gamma value 0.98 produced the maximum PSNR, suggesting better visual quality. Gamma correction, when applied consistently to all pictures, can improve overall perceptual quality and help with various image processing tasks without causing a noticeable loss in performance, even though it is computationally complex. Applying gamma correction with a value of 0.98 in the Kvasir dataset seems beneficial because it produced the highest PSNR. This implies it may improve diagnostic precision in medical imaging jobs and successfully maintain image quality.

3.5. Interpolation Technique

In this session, enlarging a picture is the process of making it larger than it is. This is frequently done to enhance an image's visual quality. Boost details that the original image could have been too tiny on. Several frequently employed interpolation techniques for picture enlargement [7] include:

10	4	2
4	22	12
3	17	32

10	*	4	*	*	2
*	*	*	*	*	*
2	*	*	22	*	12
*	*	*	*	*	*
*	*	*	*	*	*
3	*	17	*	*	32

10	10	4	4	2	2
10	10	4	4	2	2
2	2	22	22	12	12
2	2	22	22	12	12
3	3	17	17	32	32
3	3	17	17	32	32

Fig. 7 Structure of nearest neighbour of images

In order to calculate the value of each new pixel in the expanded picture, this approach chooses the value of the closest pixel in the original image. While basic nearest-neighbour interpolation, particularly when increasing photos by a significant ratio, might produce blocky or jagged edges, as shown in Figure 7. In medical pictures, enlarging the image may result in pixelation and interpolation artifacts that obscure diagnostic information. Images can become noisy and lose quality as they are enlarged, making it possible to miss important information needed for a diagnosis.

3.6. Histogram Enlargement

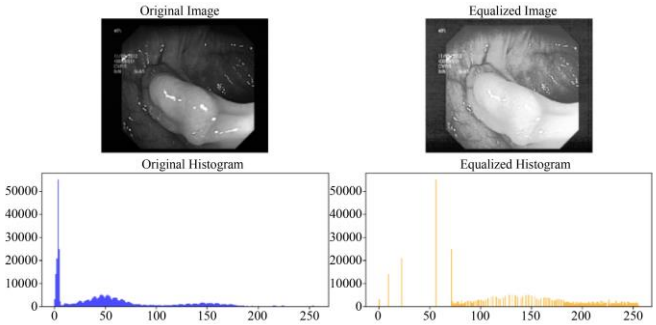

Fig. 8 Histogram enlargement applied on the kvasir Data

In this part, the goal of image processing was to enhance a picture's interpretability and visual quality. Fundamentally, this technique works using an image's histogram, which shows the distribution of pixel intensities [10]. Histogram enhancement extends an image's intensity range to cover a greater range of values by dispersing these intensity values. Through the effective enhancement of contrast between various sections of the image, details previously hidden by excessive brightness, blackness, or low contrast are now more evident. A more balanced depiction of the image's content is produced by adjusting the Cumulative Distribution Function (PDF) of the histogram using methods like histogram equalization. This produces a more consistent distribution of pixel intensities, as shown in Figure 8.

Following the use of image enlargement, the pixels of the picture tend to occupy the grey level and are uniformly distributed; this results in rich, dynamic visuals. After processing, there is a noticeable improvement in image contrast. (MSE = 5942.82, PSNR = 10.3908). While histogram expansion can improve contrast, it can also make medical pictures more noisy and prone to artifacts, which might lead to inaccurate diagnostic interpretation. Other methods that minimize noise and selectively increase contrast could be more suitable for medical imaging in specific circumstances.

3.7. Histogram Enlargement

In this area, discussed about reconstruction and the Fourier transform are useful because they may reveal important information about the frequency composition and structure of signals and pictures. Fourier analysis breaks down signals and pictures into their frequency components [11], which makes it possible to extract pertinent characteristics, find patterns, and spot abnormalities.

$$\boldsymbol{F(u,v)=\frac{1}{\sqrt{MN}}\sum_{x=0}^{M-1}\sum_{y=0}^{N-1}f(x,y)e^{j2\pi(\frac{ux}{M}+\frac{vy}{N})}}$$

$$\boldsymbol{f(x,y)\ is\ the\ original\ pixel,}$$

$$\boldsymbol{F(u,v) is\ the\ outcomes\ of\ the\ Fourier\ Transform}$$

After the four frequencies, they will meet at the center of the image, as shown in Figure 9.

$$f(x,y)(-1)^{x+y}=F\left(u-\frac{M}{2},v-\frac{N}{2}\right)$$

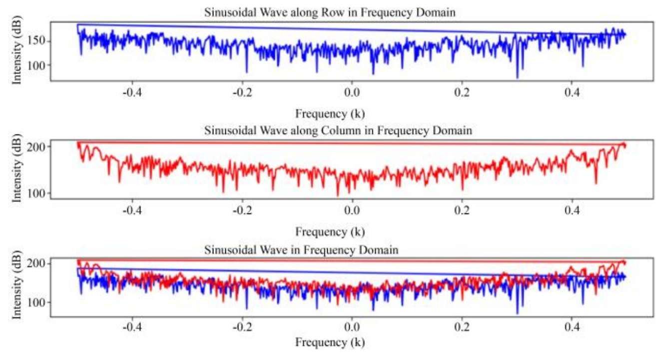

Fig. 9 Transform and reconstruction using fourier transform

DFT draws attention to the image's dominating frequencies, which are distinguished by large magnitudes in the frequency domain representation. The picture's main patterns, textures, edges, and structures match these dominating frequencies. DFT highlights periodic patterns or repeated structures in the picture, such as textures or grids, by displaying comparable peaks in the frequency domain. The image's sharp edges and changes in intensity across distinct regions are highlighted in the frequency domain shown in Figure 10. In the DFT, these edges appear as high-frequency components.

$$\boldsymbol{f(x,y)=\frac{1}{\sqrt{MN}}\sum_{u=0}^{M-1}\sum_{v=0}^{N-1}F(u,v)e^{j2\pi(\frac{ux}{M}+\frac{vy}{N})}}$$

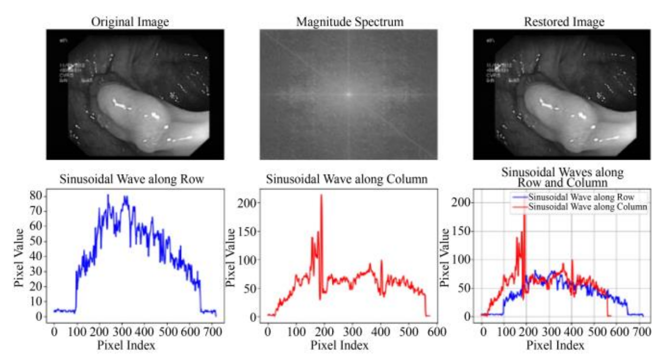

Fig. 10 Sinusoidal waves, pixel index, magnetic spectrum and restored image using DFT and IDFT analysis

IDFT emphasizes recovering fine-grained data and picture features that could have been DFT-encoded in the frequency domain. Although Fourier techniques can improve some aspects, such as spatial resolution and frequency content, their usefulness differs depending on the imaging modality and task. However, the computational complexity may be rather high, particularly when dealing with big datasets; therefore, real-time processing calls for effective algorithms and powerful computers. Overall, the needs and limitations of the current medical imaging job should be carefully considered when comparing their efficacy and computing demands.

3.8. Low Pass Filters and High Pass Filters

In this session, Low-pass filters attenuate or eliminate high-frequency components of a signal or picture while permitting low-frequency components to flow through. High-pass filters attenuate or eliminate low-frequency components of a signal or picture while permitting high-frequency components to flow through. When pictures are smoothed or blurred with LPF, noise and detail are efficiently reduced, yet low-frequency information like general brightness and large-scale structures are preserved [12]. In Figure 11, HPF is utilized to selectively highlight high-frequency information and suppress low-frequency content to improve edges and fine details.

$$\boldsymbol{H(u,v) = \frac{1}{1+[D_0/D(u,v]^{2n}}}$$

$$\boldsymbol{H(u,v) = \begin{cases} 1, D(u,v) \le D_0 \\ 0, D(u,v) > D_0 \end{cases}}$$

$\boldsymbol{D_0}$ represents the radius, D(u,v) is the distance between the two points.

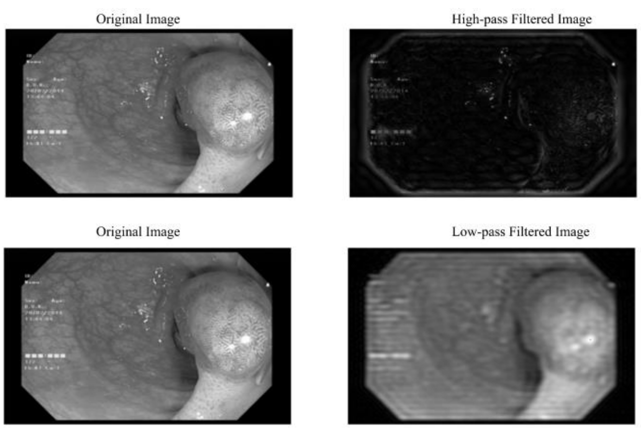

Fig. 11 Different Low & High Pass Filters

Nevertheless, a number of variables, including the imaging modality, picture properties, and filter design and parameter selection, affect how effective these filters are. The best filter combinations must be determined by careful thought and testing.

3.9. Homographic Filter

In this area, discussing about separating the components of light and reflectance [13] in a picture to improve the contrast and details. Normalizing illumination changes throughout a picture while maintaining the features seen in the reflectance component is the main objective of homomorphic filtering, shown in Figure 12. The visibility of objects and structures in photos taken in different lighting situations is improved by this normalization shown in Figure 13.

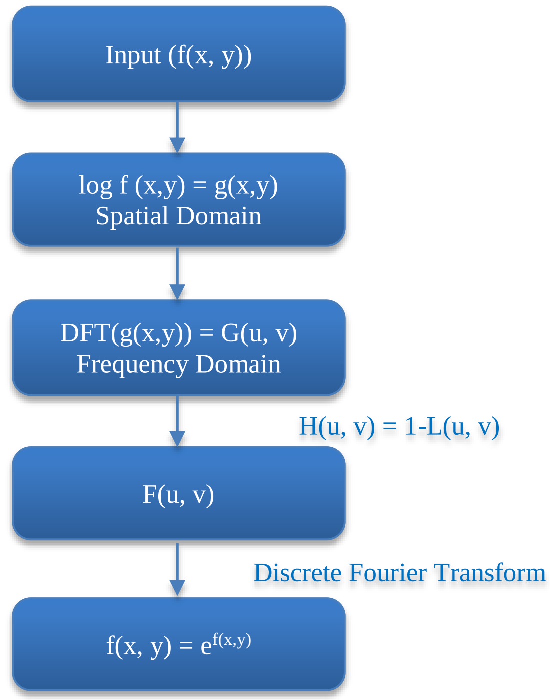

Fig. 12 Structure of homomorphic filter

$$g(x,y) = \log(1 + f(x,y)$$

$$g_{filtered}(x,y) = \exp\left(g_{filtered}(x,y)\right) - 1$$

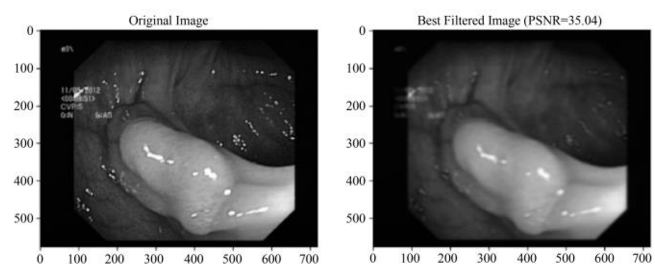

Fig. 13 Homomorphic filter applied on the kvasir data

In medical image processing, homomorphic filtering works well for improving contrast and adjusting for uneven lighting. Through the process of splitting an image into its illumination and reflectance components, homomorphic filtering can help reduce the effects of shadowing and enhance the visibility of fine features and structures in the picture. It helps improve diagnosis and analysis by boosting characteristics in photographs taken in different lighting situations or with uneven illumination.

4. Compare and Analyze the Noise Cancelling Algorithms

In this session, [14] discusses and comparing about the various noise cancelling algorithms.

4.1. Arithmetic Mean Filter

The degree of smoothing is determined by the neighbourhood's size or kernel size. While smaller areas preserve more information and somewhat decrease noise, but larger neighborhoods exhibit more noticeable smoothing effects. Because they might blur borders and features in the image, they might not be appropriate for all kinds of photos or situations when keeping little details is essential.

$$f(x, y) = \frac{1}{mn} \sum_{(s,t)\in s_{xv}} g(s, t)$$

4.2. Geometric Mean Filter

It places less weight on extreme values in the neighbourhood, and the geometric mean filter maintains edges and fine features better than the arithmetic mean filter. It may still, however, reduce noise and provide a beautiful image.

$$\boldsymbol{f(x, y) = \left[\prod_{f(s,t)\in S_{x,y}} g(s, t)\right]^{\frac{1}{mn}}}$$

4.3. Alpha-trimmed Mean Filter

"Alpha-trimmed" is a procedure whereby a certain percentage of extreme values are eliminated from a dataset to prepare it for statistical calculations like mean or median. The proportion of extreme values to be removed from each neighbourhood before calculating the mean is denoted by "alpha". The alpha-trimmed mean filter is one nonlinear image filtering method for lowering noise in photos while keeping edge details.

$$\boldsymbol{f(x, y) = \frac{1}{MN - 2d} \sum_{(x,y)\in S_{st}} g(s, t)}$$

4.4. Adaptive Mean Filter

In contrast to conventional mean filters, which compute the mean using a fixed kernel size, an adaptive mean filter dynamically modifies the neighbourhood's size according to local picture characteristics.

As a result, it can reduce noise and better retain picture features. A comparison of various noise cancellation analyses is shown in Figure 14.

Although it might blur edges, the arithmetic mean filter is straightforward and efficient for reducing noise. The Geometric Mean filter is better at preserving edges, but it might not be able to deal with sudden noise well. Alpha-trimmed filters combine edge preservation with resistance to outliers, but selecting the right parameters is crucial. The Adaptive Mean filter works well for fluctuating noise levels and keeping fine features since it modifies filter parameters locally.

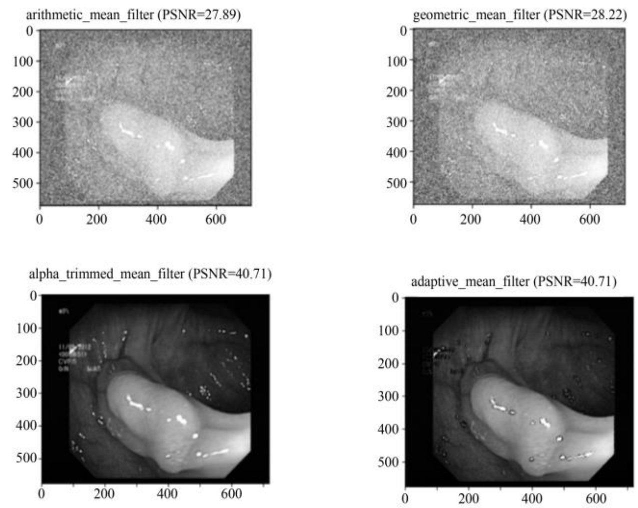

Fig. 14 Analyse and comparing of noise cancellation filters along with PSNR values

5. Compare and Analyze the Edge Detection Techniques

In this area [15], discussing and comparing about the various edge detection techniques.

In image processing, a straightforward edge detection approach is called the Roberts operator. It uses two 2x2 convolution masks to compute the image's gradient. These masks are applied to the image independently to identify the vertical and horizontal edges of the image.

$$G_x = \begin{bmatrix} 1 & 0 \\ 0 & -1 \end{bmatrix}, G_y = \begin{bmatrix} 0 & 1 \\ -1 & 0 \end{bmatrix}$$

$$G(x, y) = \sqrt{I_x(x, y)^2 + I_y(x, y)^2}$$

Prewitt computes the image's gradient to identify edges, just like the Roberts operator does. But Prewitt uses bigger convolution masks (3x3) than Roberts (2x2), which could produce edge detection results that are smoother.

$$G_x = \begin{bmatrix} -1 & 0 & 1 \\ -1 & 0 & 1 \\ -1 & 0 & 1 \end{bmatrix}, G_y = \begin{bmatrix} -1 & -1 & -1 \\ 0 & 0 & 0 \\ 1 & 1 & 1 \end{bmatrix}$$

Sobel provides superior edge localization and noise reduction compared to both the Roberts and Prewitt operators.

$$\mathbf{G_x} = \begin{bmatrix} 1 & -2 & -1 \\ 0 & 0 & 0 \\ 1 & 2 & 1 \end{bmatrix}, \mathbf{G_y} = \begin{bmatrix} -1 & 0 & 1 \\ -2 & 0 & 2 \\ -1 & 0 & 1 \end{bmatrix}$$

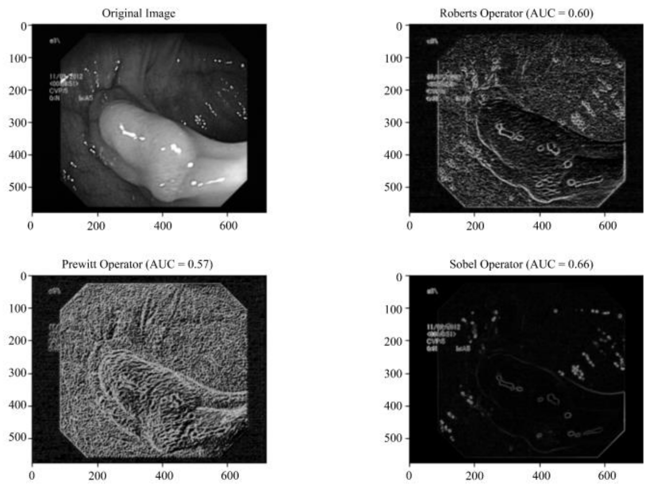

Fig. 15 Analyse and compare edge detection operators along with AUC values

The AUC may be calculated mathematically in a number of ways, including the Mann-Whitney U statistic and the trapezoidal rule. When evaluating an edge detector's capacity to accurately detect edges while reducing false positives, the AUC is a useful statistic. Better performance in differentiating between edges and non-edges is shown by higher AUC values shown in Figures 15 and 16.

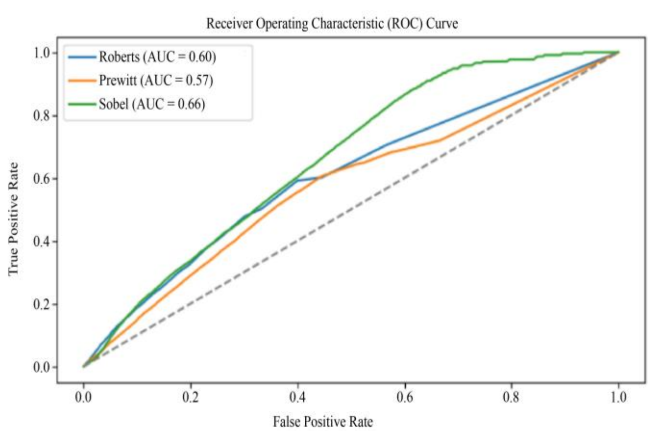

Fig. 16 Analysis using area under the curve with different edge detection operators

The Sobel filter is frequently regarded as useful for the Kvasir dataset, consisting of gastrointestinal endoscopy pictures, because of its capacity to detect edges efficiently, particularly in images with intricate textures and structures like those present in endoscopic images. The gradient-based method used in the Sobel filter can successfully draw attention to significant characteristics seen in the gastrointestinal system, such as lesions, polyps, or anomalies.

6. Analyzing the Kvasir Dataset with Interpolation Methods

This session discusses and analyses the various Interpolation methods [16] by applying them in image processing.

6.1. Adaptive Mean Filter

A straightforward interpolation method called linear interpolation is used to estimate values along a straight line between two known data points. The assumption is that there is a linear relationship between the data points.

$$y = y_1 + \frac{(x - x_1)}{(x_2 - x_1)} * (y_2 - y_1)$$

Particularly for big datasets or real-time applications with constrained computer resources, linear interpolation entails less complex computations, resulting in quicker execution times. The linearity between neighboring data points is maintained using linear interpolation. It is often less prone and more steady.

6.2. Bicubic Interpolation

The process of fitting a smooth surface to each pixel's neighborhood and using that surface to estimate the pixel's value at the target position is known as cubic interpolation. This estimate is normally carried out using bi-cubic interpolation, shown in Figure 17, using a 4x4 neighborhood of pixels.

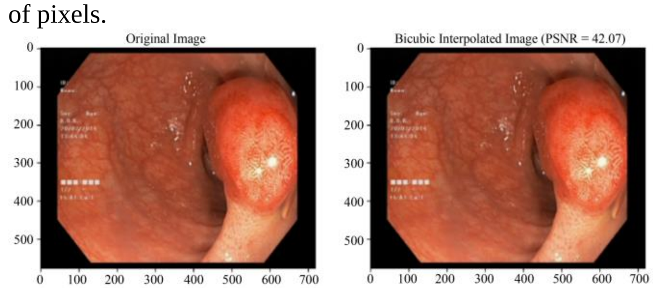

Fig. 17 Bi-cubic interpolation

7. Discussions

Coming to the discussion part, when applying an image to a picture that results in a false classification, the arithmetic and median filters, out of all the filters and approaches I covered, eliminate information from the image while smoothing it out. When certain pixel lines are missing, the image becomes jagged and blurry with smoother edges, increasing the image size but not improving its clarity in image reduction and enlargement. By removing the fuzzy (dark and bright portions) and highlighting the photos, gamma correction—a nonlinear color editing technique—alters the contrast of the photographs while still being effective. However, the computational complexity was quite high, and the datasets would vary in how the gamma value variance is changed. In a histogram enlargement, the image's pixels are uniformly distributed and tend to occupy the whole grayscale. As a result, the picture contrast is improved following processing since the grey details tend to be rich, and the dynamic range is wide. However, the event-based distribution of the pixels has changed the pixels in this instance. When evaluating DFT and IDFT, the algorithm's time complexity increases, and its execution speed becomes quite sluggish when working with big datasets. After the picture is inverted and Fourier transformed, it is confirmed that the original image is recovered. Completely reject all frequency signals over the cut-off frequency on the low-pass and high-pass filters, and vice versa. So, the picture becomes hazy. Two different sorts of activities occur when anything enters the homomorphic filtering: the illumination component and the 2. reflectance part. It quickly modifies the portion and focuses on the high-frequency pictures, and vice versa, adjusting the images on their own. However, there are pixel-by-pixel alterations and features lost. Compared to other filters, the adaptive mean filter performs best, although alpha-trimmed filtering removes noise from photos contaminated by salt and pepper. However, you would want to change the k_size and alpha_size settings. Enhancing the alpha size improves the image score (PSNR). The margins of the pictures in Roberts will become closer to either +45 or -45 degrees.

On the edges, it has a great positioning precision. The Prewitt operator works well for detecting grayscale gradients and pictures with higher noise; however, it is inappropriate for edges. Finding edges based on how close an edge is to its extreme value based on the weighted difference (Sobel) of its neighbor's intensity. Sobel is superior to all other edge detection and noise reduction filters because it combines the noise resistance and Gaussian smoothening outcomes.

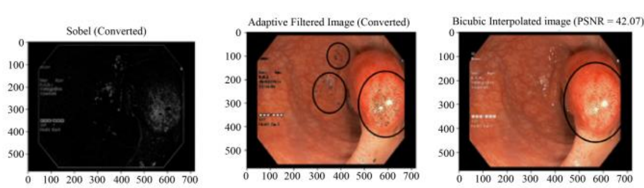

Fig. 18 Comparative Analysis of Gamma Correction + Adaptive Filter and Bi-cubic Interpolation

A comparison between a combined filter and bicubic interpolation is shown in Figure 18. Better outcomes were obtained with a 3x3 kernel for the adaptive filter, a kernel size of 15, and a Gamma value of 0.98. The combined filter's PSNR values were significantly higher-49.44 than those of the bicubic interpolation method, which was 42.06. Furthermore, the MSE values showed a notable improvement, with the combined filter receiving a score of 0.73 as opposed to 4.04 for Bicubic Interpolation. This implies that the combined filter technique fared better than bicubic interpolation in terms of improving picture quality.

8. Conclusion

By modifying the parameters, the Gamma Correction works well in the setting of the Kvasir dataset, which includes gastrointestinal endoscopic pictures for various disorders such as polyps, ulcerative colitis, and esophagitis. The Adaptive Mean Filter may successfully minimize such noise while maintaining the clarity of edges and features in the picture. Sobel edge detection is important in recognizing edges and boundaries within endoscopic images. Sometimes, it leads to complexity when dealing with complex datasets. Our investigation shows that sophisticated mathematical methods may effectively improve Lower Gastrointestinal (GI) tract photographs, such as those showing pylorus, normal-cecum, and ulcerative colitis. We significantly improved the image quality by integrating Gaussian functions, Fast Fourier Transform (FFT), Inverse Fast Fourier Transform (IFFT), and numerous statistical filters. Notably, the classic bi-cubic filter was significantly outperformed by combining Gaussian correction and adaptive mean filtering. In contrast to the bi-cubic filter's 42.06 PSNR and 4.04 MSE, this combined technique produced a Peak Signal-to-Noise Ratio (PSNR) of 49.44 and a Mean Squared Error (MSE) of 0.73. These results demonstrate how the adaptive mean filter and Gaussian correction technique may work together to improve classification and detection accuracy by producing more clarity and detailed images.

Future developments will see SRRNet and SRGAN surpass standard filters in producing higher-resolution pictures with more precise details, better perceptual quality, fewer artifacts, and versatility to accommodate different image content and styles. They mark a major advancement in image-enhancing methods, especially for fields like satellite imagery, medical imaging, and photography, where crisp images are crucial.

Funding Statement

This research is supported by the Basic Science Research Program through the National Research Foundation of Korea (NRF), funded by the Ministry of Education (NRF- RS-2023-00237287).

Data Availability Statement

The datasets used and/or analyzed during the current study are available from the corresponding author upon reasonable request.

References

[1] Peng Si et al., "Feature Context Aggregation Network with Edge Enhance for Endoscopic Gastrointestinal Bleeding Images Segmentation," *IEEE 10th Data Driven Control and Learning Systems Conference*, Suzhou, China, pp. 77-81, 2021. [CrossRef] [Google Scholar] [Publisher Link]

[2] T.K. Kho, K.S. Sim, and F.F. Ting, "Gastrointestinal Endoscopy Colour-Based Image Processing Technique for Bleeding, Lesion and Reflux," *International Conference on Robotics, Automation and Sciences*, Melaka, Malaysia, pp. 1-4, 2016. [CrossRef] [Google Scholar] [Publisher Link]

[3] Yassine Oukdach et al., "ConV-ViT: Feature Fusion-Based Detection of Gastrointestinal Abnormalities Using CNN and ViT in WCE Images," *10th International Conference on Wireless Networks and Mobile Communications*, Istanbul, Turkiye, pp. 1-6, 2023. [CrossRef] [Google Scholar] [Publisher Link]

[4] Dev Gupta et al., "Classification of Endoscopic Images and Identification of Gastrointestinal Diseases," *International Conference on Machine Learning, Big Data, Cloud and Parallel Computing*, Faridabad, India, pp. 231-235, 2022. [CrossRef] [Google Scholar] [Publisher Link]

[5] Zhenwei Miao, and Xudong Jiang, "Further Properties and a Fast Realization of the Iterative Truncated Arithmetic Mean Filter," *IEEE Transactions on Circuits and Systems II: Express Briefs*, vol. 59, no. 11, pp. 810-814, 2012. [CrossRef] [Google Scholar] [Publisher Link]

[6] Qing Lyu et al., "Cine Cardiac MRI Motion Artifact Reduction Using a Recurrent Neural Network," *IEEE Transactions on Medical Imaging*, vol. 40, no. 8, pp. 2170-2181, 2021. [CrossRef] [Google Scholar] [Publisher Link]

[7] M.Z.F. Amara, R. Bandara, and Thushari Silva, "SLIC Based Digital Image Enlargement," *18th International Conference on Advances in ICT for Emerging Regions*, Colombo, Sri Lanka, pp. 1-6, 2018. [CrossRef] [Google Scholar] [Publisher Link]

[8] Fathi Kallel, and Ahmed Ben Hamida, "A New Adaptive Gamma Correction Based Algorithm Using DWT-SVD for Non-Contrast CT Image Enhancement," *IEEE Transactions on NanoBioscience*, vol. 16, no. 8, pp. 666-675, 2017. [CrossRef] [Google Scholar] [Publisher Link]

[9] Sijin Li et al., "Color Bleeding Reduction in Images and Video Compression," *Proceedings of 2011 International Conference on Computer Science and Network Technology*, Harbin, China, 2011. [CrossRef] [Google Scholar] [Publisher Link]

[10] Ningxiong Mao et al., "Reversible Data Hiding of JPEG Image Based on Adaptive Frequency Band Length," *IEEE Transactions on Circuits and Systems for Video Technology*, vol. 33, no. 12, pp. 7212-7223, 2023. [CrossRef] [Google Scholar] [Publisher Link]

[11] Shekhar S. Chandra et al., "Robust Digital Image Reconstruction via the Discrete Fourier Slice Theorem," *IEEE Signal Processing Letters*, vol. 21, no. 6, pp. 682-686, 2014. [CrossRef] [Google Scholar] [Publisher Link]

[12] Paul D. Laforge, Raafat R. Mansour, and Ming Yu, "The Use of Low-Pass Filters as Impedance Inverters for Highly Miniaturized Superconducting Bandstop Filter Designs," *IEEE Transactions on Applied Superconductivity*, vol. 21, no. 3, pp. 575-578, 2011. [CrossRef] [Google Scholar] [Publisher Link]

[13] Ángel Chavarín et al., "Contrast Enhancement in Images by Homomorphic Filtering and Cluster-Chaotic Optimization," *IEEE Access*, vol. 11, pp. 73803-73822, 2023. [CrossRef] [Google Scholar] [Publisher Link]

[14] Hsing-Yen Tsai et al., "3-D Wireless Power Transfer With Noise Cancellation Technique for −62-dB Noise Suppression and 90.1% Efficiency," *IEEE Solid-State Circuits Letters*, vol. 6, pp. 213-216, 2023. [CrossRef] [Google Scholar] [Publisher Link]

[15] Ahmed H. Abdel-Gawad, Lobna A. Said, and Ahmed G. Radwan, "Optimized Edge Detection Technique for Brain Tumor Detection in MR Images," *IEEE Access*, vol. 8, pp. 136243-136259, 2020. [CrossRef] [Google Scholar] [Publisher Link]

[16] G.J. Grevera, J.K. Udupa, and Y. Miki, "A Task-Specific Evaluation of Three-Dimensional Image Interpolation Techniques," *IEEE Transactions on Medical Imaging*, vol. 18, no. 2, pp. 137-143, 1999. [CrossRef] [Google Scholar] [Publisher Link]